J Therm Anal Calorim (2010) 99:887–892
DOI 10.1007/s10973-010-0680-5

Solid–liquid phase diagrams of binary mixtures

Acetylsalicylic acid(1) + E(2) (E = salicylic acid, polyethylene glycol 4000, D-mannitol)

Luigi Campanella · Valentina Micieli · Mauro Tomassetti · Stefano Vecchio

MEDICTA2009 Special Issue

Abstract This study reports the investigation of three binary mixtures represented by acetylsalicylic acid (ASA) with its most important degradation product, salicylic acid (SA), and two of the most commonly used excipients (polyethylene glycol 4000 (PEG-4000) and D-mannitol (MA)). The liquidus and solidus equilibrium temperatures determined by DSC for pure components and solid binary mixtures at a fixed composition (mass fraction of ASA, w) were used to construct the corresponding solid–liquid phase diagrams. On the basis of the DSC results, the binary mixtures ASA/SA and ASA/PEG exhibit eutectic behavior ($T_{eu} = 155.0 \pm 0.5$ °C, $w_{eu} = 0.55 \pm 0.02$ and $T_{eu} = 53.3 \pm 0.5$ °C, $w_{eu} = 0.327 \pm 0.011$), respectively), while the binary mixture ASA/MA revealed the presence of a monotectic with a mean melting temperature of 162.2 °C in the range $0.2 < w_1 < 0.8$. The composition of the two eutectics formed was confirmed by the related Tamman triangles. Finally, the liquidus curves of ASA/SA and ASA/PEG mixtures were also successfully predicted providing suitable polynomial (second-order) fitting equations.

Keywords Acetylsalicylic acid · DSC · D-mannitol · Eutectic composition · PEG-4000 · Phase diagrams · Salicylic acid · Second-order fitting equation

L. Campanella · M. Tomassetti
Department of Chemistry, Sapienza University of Rome, P.le A. Moro, 5, 00185 Rome, Italy

V. Micieli · S. Vecchio (✉)
Department of Chemical Engineering Materials and Environment, Sapienza University of Rome, Via del Castro Laurenziano 7, 00161 Rome, Italy
e-mail: stefano.vecchio@uniroma1.it

Introduction

Since the beginning of the twentieth century, acetylsalicylic acid (ASA) was considered one of the first anti-inflammatory nonsteroidal drugs used in clinical practice. Up to now, it is the most widely used analgesic, antipyretic, anti-inflammatory drug and is taken as the term of comparison for evaluating and comparing other peripheral analgesics. Differential scanning calorimetry (DSC) is one of the most effective and used technique to distinguish whether binary mixtures form solid solutions or eutectic systems [1] and to monitor a liquid–solid phase diagram for binary organic and inorganic systems [2–9], in particular in the pharmaceutical field for active component/excipients binary systems [10–12]. Several authors found that ASA forms eutectic mixtures with many components, like acetaminophen [13, 14], propoxyphene HCl [15], phenobarbital [16], and urea [13]. Some years ago, Becket and coworkers found in binary mixtures with high percentage of ASA a linear correlation between temperatures and fusion enthalpies of ASA and those of salicylic acid (SA) [17]. In addition, ASA is known to form a eutectic with SA [18], the main metabolite resulting from its hydrolysis, although as far as the exact percentages are concerned, and to a lesser extent the exact eutectic temperature, is not known.

Nowadays, polyethylene glycols have been extensively used as solid dispersion carriers because of their low melting temperatures, rapid solidification rate and low toxicity and economic cost, while D-mannitol is recognized to be one of the most popular substances for a solid dispersion matrix among sugars due to its very low toxicity and high aqueous solubility [2].

In this study, the thermal behavior of binary mixtures represented by ASA with SA and two of the most

commonly used excipients (polyethylene glycol 4000 (PEG-4000) and D-mannitol (MA)) was examined using DSC with a view to construct the corresponding binary phase diagrams.

Experimental and methods

Materials

Acetylsalicylic acids, salicylic acid, polyethylene glycol 4000 were supplied by Fluka, while D-mannitol by Carlo Erba Reagents. Since purity of all products, certified by the suppliers, resulted to be over 97%, w/w, they were used without further purification. The procedure adopted in this study before carrying out the DSC experiments consists of preparing a series of solid binary mixtures (with compositions, expressed as mass fraction of ASA w_1, covering the whole composition range) by gently blending the appropriate quantities of pure components in a agate mortar for about 10 min. All pure components were also ground up in an agate mortar using the same procedure.

Determination of experimental and predicted phase transition temperatures and eutectic compositions

The DSC measurements were carried out on a simultaneous Stanton Redcroft STA 625 TG/DSC thermoanalyzer, connected to a 386 IBM-compatible personal computer. Thermodynamic quantities were calculated using the Stanton-Redcroft Data Acquisition System, Trace 2, Version 4. Temperature and heat flow rate scales were calibrated with very pure standards (indium, lead, tin, zinc), whose melting temperatures and enthalpies are well known [19]. Samples of about 10 mg were weighed into Al pans in an argon-filled dry box to avoid a possible sample degradation, and then in the thermoanalyzer, where the purge air stream fluxed to continuously remove the gases given off during the thermal heating process experiment. Three DSC experiments were made for each sample at 2 K min^{-1} using fresh product only. The phase transition temperatures of the samples were measured during the first heating (evaluated as onset DSC peak temperatures) because the use of resolidified melts was unacceptable due to the possibility of polymorphic changes and the corresponding phase diagrams were obtained when these experimental temperatures were properly interpreted and connected (interpolated) to form phase lines [20]. Unfortunately, for a eutectic binary system in which two phase lines converge to the same temperature at a particular composition (eutectic composition) its correct estimation was usually difficult with the use of conventional DSC equipment for several reasons [2]. The accuracy associated

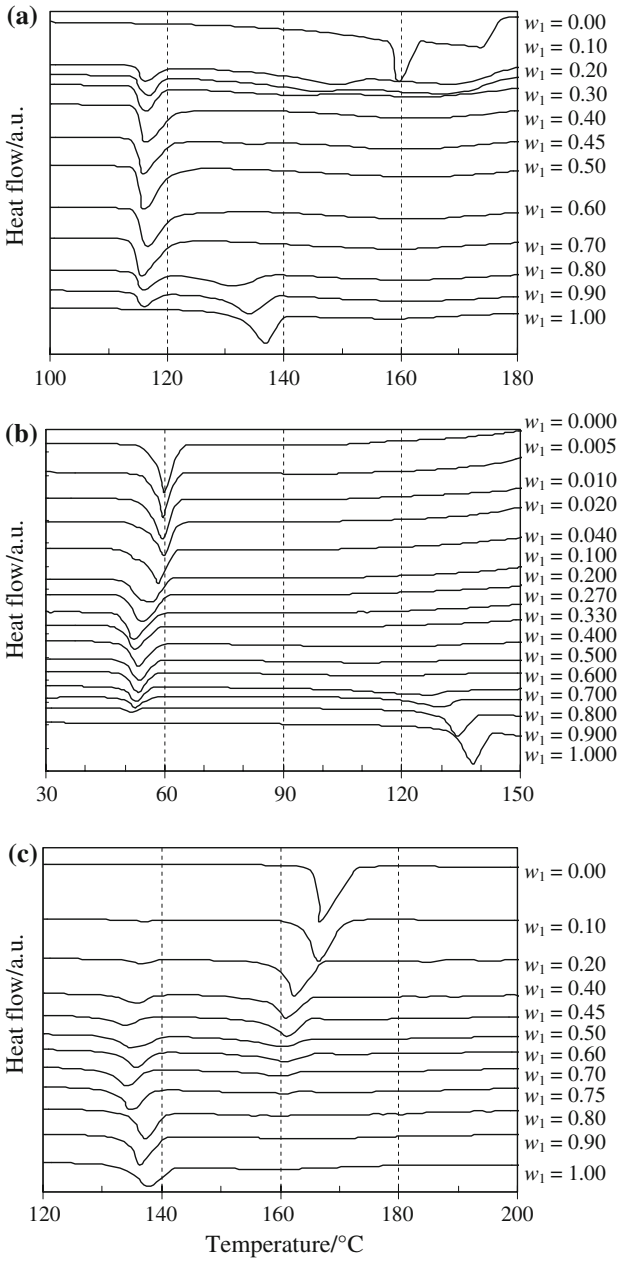

Fig. 1 DSC curves at heating rate of 2 K min^{-1} under a stream of air of binary mixtures: **a** ASA/SA, **b** ASA/PEG-4000, and **c** ASA/MA. The composition (on the *right side* of the plots) is expressed in mass fraction of ASA (w_1)

to the determination of the eutectic composition can be significantly improved using the enthalpic method [9, 21–23]. This approach is based on the composition dependence of the eutectic melting enthalpy in the form of the well-known Tamman's triangle, where the maximum value of the eutectic melting enthalpy is obtained for the mass fraction corresponding to the eutectic composition w_{eu}. To this end, the experimental heat flux versus temperature data points were fitted to multiple nonlinear regression equation using Gaussian and exponentially

modified Gaussian peaks for deconvolution of symmetric and asymmetric DSC melting peaks, respectively. The details of the mathematical procedure adopted are reported in the literature [23].

Results and discussion

Before construction of the binary phase diagrams, all the DSC curves are given in Fig. 1a–c. SA is the only pure component that showed (Fig. 1a) two endothermic peaks in the temperature range investigated, ascribable to melting followed by vaporization. For the other pure components only one melting DSC peak is found, while two melting DSC peaks were observed in all the cases for the binary mixtures ASA/excipients (E) up to 473 K, being the first one, at lower temperature, attributable to the melting of eutectic (Fig. 1a–b) or monotectic system (Fig. 1c), while the second one, at higher temperature, corresponds to melting of the major component.

The experimental melting point values (T_{fus}) of the pure components and of the respective binary mixtures are reported in Table 1, and plotted in Figs. 2a, 3a, and 4. In particular, the melting temperatures of pure ASA, SA, PEG, and MA were found to be 135.6 ± 0.5, 160.3 ± 0.5, 59.9 ± 0.5, and 166.9 ± 0.5 °C, respectively. The enthalpies of fusion of the pure components and of the respective binary mixtures (except for the ASA/MA binary mixtures) were also summarized in Table 1 for each given ASA mass fraction value, w_1. In particular, the enthalpies of fusion of pure ASA, SA, PEG, and MA were found to be 106 ± 2, 93 ± 2, 178 ± 5, and 184 ± 3 J g^{-1}, respectively.

The phase diagrams reported in the plots *a* of Figs. 2 and 3 clearly show that ASA/SA and ASA/PEG-4000 binary mixtures exhibit a simple eutectic behavior. After deconvolution of the melting endothermic DSC peaks using a multiple nonlinear regression method, the compositional dependence of the enthalpy of fusion so obtained was determined for the component in excess. From the characteristic Tamman's triangle shape obtained after a linear regression of the enthalpy of fusion (after deconvolution) versus w_1 data points (plots *b* of Figs. 2, 3), the temperatures and compositions of the ASA/SA and ASA/PEG-4000 eutectics systems (expressed as mass fraction), were accurately determined: $T_{eu} = 155.0 \pm 0.5$ °C, $w_{eu} = 0.55 \pm 0.02$ and $T_{eu} = 53.3 \pm 0.5$ °C, $w_{eu} = 0.327 \pm 0.011$, respectively. The uncertainty associated to each eutectic temperature is equal to the experimental error

Table 1 Melting temperatures and enthalpies of the binary system ASA (w_1) + E ($1 - w_1$), where E = SA, PEG-4000, and MA

w_1	ASA/SA mixture			ASA/PEG-4000 mixture			ASA/MA mixture	
	1st DSC peak		2nd DSC peak	1st DSC peak		2nd DSC peak	1st DSC peak	2nd DSC peak
	T/°C[a]	ΔH/J g^{-1}[a]	T/°C[a]	T/°C[a]	ΔH/J g^{-1}[a]	T/°C[a]	T/°C[a]	T/°C[a]
0.000	160.3	93	–	59.9	178	–	166.9	–
0.005	–	–	–	59.9	21	–	–	–
0.010	–	–	–	59.7	21	–	–	–
0.020	–	–	–	55.3	21	59.5	–	–
0.100	116.2	35	157.9	51.9	37	59.3	131.4	166.1
0.200	115.4	55	152.7	51.4	53	56.9	131.4	162.7
0.270	–	–	–	51.4	53	56.9	–	–
0.300	114.4	83	144.9	–	77	54.3	–	161.7
0.330	–	–	–	–	77	54.3	–	–
0.400	115.9	105	135.8	53.9	72	88.7	129.4	161.3
0.450	114.3	–	–	54.3	–	–	126.9	161.1
0.500	114.3	–	–	–	61	108.3	131.3	160.0
0.550	–	–	–	54.1	55		131.2	160.6
0.600	116.1	124	120.9	53.9	49	120.9	129.0	160.5
0.700	114.4	100	129.8	53.5	37	128.5	131.8	160.3
0.750	–	–	–	–	–	–	134.5	159.2
0.800	114.6	58	132.2	51.9	26	132.2	134.5	159.2
0.900	116.2	33	134.6	55.3	14	135.4	134.4	
1.000	135.6	106	–	135.6	106	–	135.6	–

[a] The temperature uncertainty is ±0.5 °C, while the enthalpy uncertainty is always lower than 7%

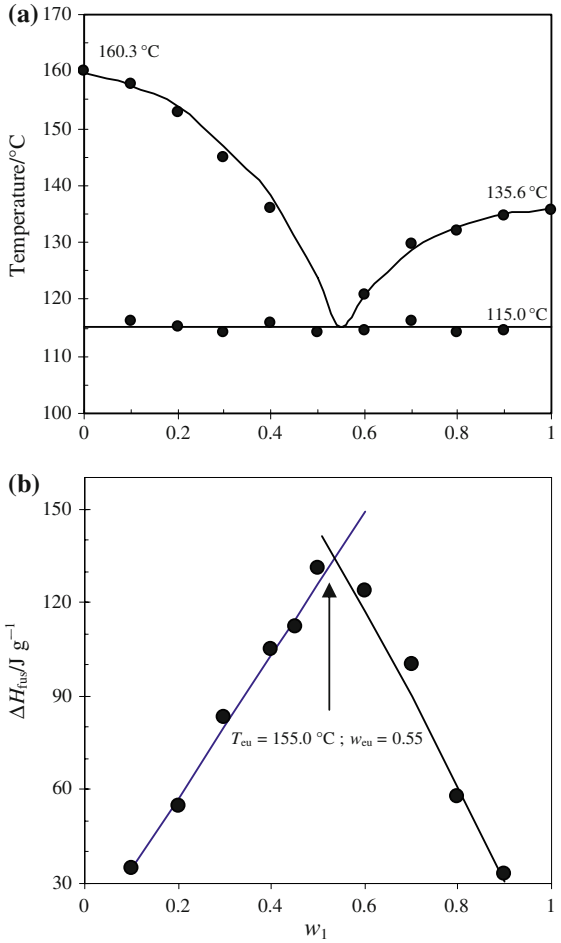

Fig. 2 **a** Solid–liquid phase diagram of the binary system ASA(1) + SA(2), *filled circle* experimental values, *line* predicted liquidus lines according to Eq. 2 whose fitting parameters are reported in Table 2 and **b** Tamman plot of the binary system ASA/SA

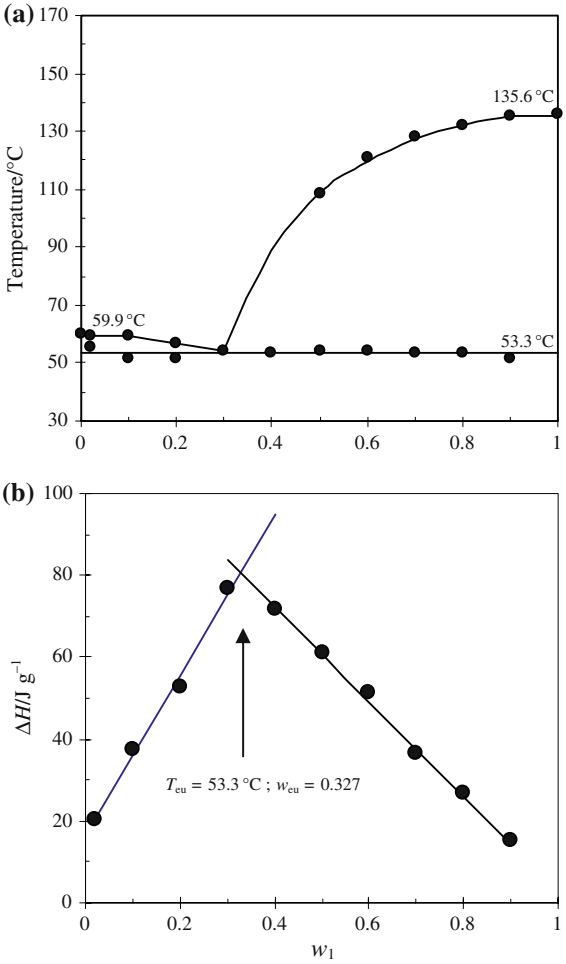

Fig. 3 **a** Solid–liquid phase diagram of the binary system ASA(1) + PEG-4000(2), *filled circle* experimental values, *line* predicted liquidus lines according to Eq. 2 whose fitting parameters are reported in Table 2 and **b** Tamman plot of the binary system ASA/PEG-4000

associated to the measured sample temperatures, while those associated to the mass fraction were estimated from uncertainties associated to the slopes of both the regression lines in the Tamman's plots.

The two branches of the liquidus curves of both the binary systems ASA/SA and ASA/PEG-4000 with compositions $w_1 < w_{eu}$ and $w_1 > w_{eu}$, respectively, represented in Figs. 2a and 3a by the measured melting temperatures T_{fus} versus w_1 experimental data, were subsequently interpolated using the Schröder–van Laar equation [24]:

$$-\ln(x_i) = \Delta H_{fus}/R(1/T - 1/T_i) \quad (1)$$

where x_i, ΔH_{fus}, and T_i are, respectively, the molar fraction, the enthalpy of fusion, and the melting temperature of the component in excess. Fitting experimental data to Eq. 1 results to be unsuccessful because of the large deviation from ideality of the ASA/SA and ASA/PEG-4000 systems in the molten state. Therefore, it was decided to interpolate

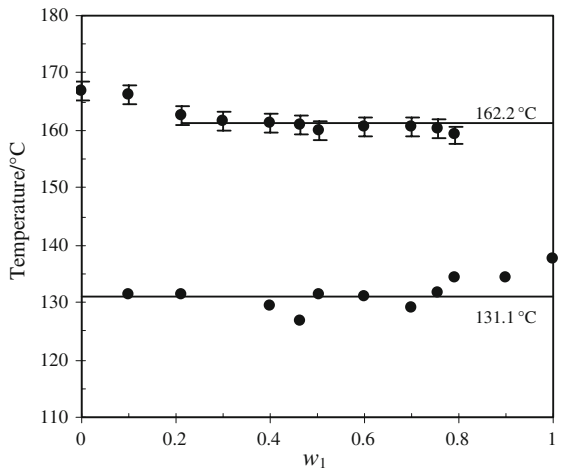

Fig. 4 Solid–liquid phase diagram of the binary system ASA(1) + MA(2), *filled circle* experimental values, and *line* mean of values in the range $0.2 \leq w_1 \leq 1.0$

Table 2 Parameters of second-order equations $T_{fus}(^{\circ}C) = a \cdot w_1^2 + b \cdot w_1 + c$ for fitting experimental T_{fus} vs. w_1 data

Binary system	Range of w_1	a/°C[a]	b/°C[a]	c/°C[a]	R^2
ASA/SA	<0.55	−144.5	2.76	159.2	0.9981
ASA/SA	>0.55	−132.0	248.2	19.0	0.9950
ASA/PEG-4000	<0.30	−27.6	−12.5	60.5	0.9875
ASA/PEG-4000	>0.30	−236.3	413.7	−43.2	0.9815

[a] Uncertainties associated to fitting parameters are always lower than 8%

The number of digits of fitting parameters depends on the corresponding uncertainty

the melting temperatures T_{fus} versus w_1 experimental data, using a polynomial (second-order) fitting equation, which has the following usual form:

$$T_{fus}(^{\circ}C) = a \cdot w_1^2 + b \cdot w_1 + c \quad (2)$$

The fitting parameters a, b, and c and the squares of the correlation coefficients (R^2), obtained using a nonlinear regression based on the least square method, were reported in Table 2. Estimated uncertainties associated to fitting parameters, expressed in terms of percentages of relative standard deviations, are found always lower than 8%. For both ASA/SA and ASA/PEG-4000 binary mixtures the corresponding liquidus lines, predicted using Eq. 2, were displayed in Figs. 2a and 3a (solid lines). Lastly, as far as the binary system ASA/MA is concerned (whose phase diagram is displayed in Fig. 4), the melting temperatures of each component do not change significantly over the entire range of composition: practically constant melting temperatures were observed in the range $0.2 < w_1 < 0.8$ (within the experimental uncertainties, reported as error bars in Fig. 4) with a mean value of 162.2 °C, thus suggesting that the ASA/MA system follows a monotectic behavior. Only a slight decreasing trend was observed for the melting temperature of MA of up to $w_1 = 0.2$, already observed in the literature in other binary system containing MA [2, 24, 25] and sometimes ascribed to the presence of possible metastable modifications [2]. Finally, for the ASA/MA system the isotherm corresponding to the mean temperature value was reported in Fig. 4.

In conclusion, the confirmation of the presence of a eutectic between ASA and SA is of considerable practical importance in the pharmaceutical field considering the frequency with which the presence of salicylic acid impurities in ASA-based pharmaceutical formulations is detected due to the tendency of this active principle to undergo hydrolysis.

Acknowledgements This study was funded by "Sapienza University of Rome," "Ateneo and University Projects."

References

1. Young PH, Dollimore D, Schall CA. Thermal analysis of solid-solid interactions in binary mixtures of alkylcyclohexanes using DSC. J Therm Anal Calorim. 2000;62:163–71.
2. Zajc N, Srčič S. Binary melting phase diagrams of nifedipine-PEG 4000 and nifedipine-mannitol systems. J Therm Anal Calorim. 2004;77:571–80.
3. Ding MS, Xu K, Jow TR. Phase diagrams of EC-DMC binary system and enthalpic determination of its eutectic composition. J Therm Anal Calorim. 2000;62:177–86.
4. Wojakowska A, Górniak A, Wojakowski A. Thermodynamics and equilibrium phase diagrams of the zinc halide + silver halide system. J Chem Eng Data. 2004;49:1231–5.
5. Costa MC, Rolemberg MP, Boros LAD, Krähenbühl MA, de Oliveira MG, Meirelles JA. Solid-liquid equilibrium of binary fatty acid mixtures. J Chem Eng Data. 2007;52:30–6.
6. Kuhnert-Brandstätter M, Burger A. Phase diagrams of urea inclusion compounds 3. pentadecanoid acid and urea. J Therm Anal. 1998;52:315–25.
7. Rai US, Pandey P, Rai RN. Physical chemistry of binary organic eutectic and monotectic alloys; 1, 2, 4, 5-tetrachlorobenzene-α-naftol and TCB-resorcinol systems. Mat Lett. 2002;53:83–90.
8. Weise S, Krämer V. Phase study of the system Li_2Se-In_2Se_3. J Therm Anal Calorim. 2003;71:1035–8.
9. Zhang L, Ueno S, Sato K, Adlof RO, List GR. Thermal and structural properties of binary mixture of 1,3-distearoyl-2-oleoyl-glycerol (SOS) and 1, 2-dioleoyl-3-stearoyl-sn-glycerol (sn-OOS). J Therm Anal Calorim. 2009;98:105–11.
10. Ginés JM, Arias MJ, Moyano JR, Novak Cs, Pokol G, Sánchez-Soto PJ. Thermal investigation of PEG 4000–oxazepam binary system. J Therm Anal. 1996;47:1743–53.
11. Bartsch SE, Griesser UJ. Physicochemical properties of the binary system glibenclamide and polyethylene glycol 4000. J Therm Anal Calorim. 2004;77:555–69.
12. Law D, Wang W, Schmitt EA, Long MA. Prediction of poly(ethylene) glycol-drug eutectic compositions using an index based on the van't Hoff equation. Pharm Res. 2002;19:315–21.
13. el-Banna HM. Solid dispersion of pharmaceutical ternary systems I: phase diagram of aspirin-acetaminophen-urea system. J Pharm Sci. 1978;67:1109–11.
14. Muller BW, Beer Y. Polymorphie und Trachtänderung von Propyphenazon. Acta Pharm Tech. 1982;28:97–102.
15. Law SL, Lo WY, Lin FM, Chiang CH. Compatibility study of propoxyphene HCL solid mixtures using differential scanning calorimetry. Drug Dev Ind Pharm. 1988;14:1465–70.
16. Sangster J. Phase diagrams and thermodynamic properties of binary systems of drugs. J Phys Chem Ref. 1999;28:889–929.
17. Becket G, Quah SB, Hill JO. A DSC compositional analysis of some binary organic mixtures of pharmaceutical significance. J Therm Anal. 1993;40:537–42.
18. Ceschel GC, Badiello R, Ronchi C, Maffei P. Degradation of components in drug formulations: a comparison between HPLC and DSC methods. J Pharm Biomed Anal. 2003;32:1067–72.
19. Hultgren R, Desai PD, Hawkins DT, Gleiser M, Kelley KK, Wagman DD. Selected values of the thermodynamic properties of the element. Metals Park, OH: American Society for Metals; 1973.
20. Sestak J. Thermophysical properties of solids. Their measurements and theoretical thermal analysis, Comprehensive Analytical Chemistry. Vol. XII. Prague: G. Svehla; 1984. p. 116–126.
21. Olkhovaya LA, Fedorov PP, Ikrami DD, Sobolev BP. Phase diagrams of MgF_2-(Y, Ln)F_3 systems. J Therm Anal. 1979;15:355–60.

22. Maciejewski M, Brunner TJ, Loher SF, Stark WJ, Baiker A. Phase transitions in amorphous calcium phosphates with different Ca/P ratios. Thermochim Acta. 2008;468:75–80.
23. Prankerd RJ, Elsabee MZ. Thermal analysis of chiral drug mixtures: the DSC behaviour of mixtures of ephedrine HCl and pseudoephedrine HCl enantiomers. Thermochim Acta. 1995;248: 147–60.
24. Telang C, Suryanarayanan R, Yu L. Effective inhibition of mannitol crystallization in frozen solutions by sodium chloride. Pharm Res. 2003;20:1939–45.
25. Siniti M, Jabrane S, Létoffé JM. Study of the respective binary phase diagrams of sorbitol with mannitol, maltitol and water. Thermochim Acta. 1999;325:171–80.